

Extraction of Neutrino Oscillation Parameters Using Negative Log-Likelihood Fitting

Mohammed Zain Mughal, CID: 02203769

Abstract—The physical phenomenon of neutrino oscillations provides key insights into the properties of neutrinos, particularly their masses and mixing angles, and far beyond this. This comprehensive study dives into employing computational methods to extract key oscillation parameters, θ_{23} and Δm^2 , using synthetic representative observed event counts and a theoretical oscillation model. Negative Log-Likelihood (NLL) techniques, including Grid Search, Simulated Annealing, and Nelder-Mead, are implemented to optimize parameter estimated fits. We introduce detector resolution effects via Gaussian smearing alongside Fourier convolution cross-validation, whilst accounting for cross-section uncertainties with a scaling factor α , to refine parameter estimates. The Nelder-Mead minimization method yielded the best results, achieving a best-fit value of $\theta_{23} = 0.685 \pm 0.02$ and $\Delta m_{23}^2 = 0.0022378 \pm 0.01$ eV². By evaluating validations between methods and analyzing residuals for robustness within the systematic effects mitigated by smearing and scaling adjustments. This report breaks down a detailed evaluation of computational techniques and the resultant implications on the field of neutrino physics.

I. INTRODUCTION

Neutrino oscillations were a groundbreaking discovery in the space of particle physics, they occur due to the quantum mechanical interaction where neutrino flavor eigenstates (ν_e, ν_μ, ν_τ) are superpositions of mass eigenstates (ν_1, ν_2, ν_3), this behavior is direct evidence for non-zero neutrino masses, challenging the assumption of massless neutrinos in the Standard Model of Particle Physics. The probability of a neutrino transitioning from one flavor state (ν_α) to another (ν_β) as it propagates through space is given by: [5]

$$P_{\nu_\alpha \rightarrow \nu_\beta} = \delta_{\alpha\beta} - 4 \sum_{i>j} \text{Re} (U_{\alpha i} U_{\beta i}^* U_{\alpha j}^* U_{\beta j}) \sin^2 \left(\frac{\Delta m_{ij}^2 L}{4E} \right) \quad (1)$$

where $U_{\alpha i}$ are the elements of the Pontecorvo–Maki–Nakagawa–Sakata (PMNS) matrix, Δm_{ij}^2 represents the mass-squared differences between mass eigenstates, L is the baseline (distance traveled by the neutrino), and E is the neutrino energy [5]. For atmospheric neutrinos, where oscillations are dominated by the $\nu_\mu \leftrightarrow \nu_\tau$ channel, this simplifies to:

$$P_{\nu_\mu \rightarrow \nu_\tau} = \sin^2(2\theta_{23}) \sin^2 \left(1.27 \frac{\Delta m_{23}^2 L}{E} \right), \quad (2)$$

where θ_{23} is the mixing angle and Δm_{23}^2 is the dominant mass-squared difference. Determining these parameters is crucial for advancing our understanding of neutrino properties and the underlying physics beyond the Standard Model of the universe.

The objectives of this comprehensive study are to determine the best-fit values for θ_{23} and Δm_{23}^2 by leveraging minimisation techniques on the Negative Log-Likelihood (NLL) function, evaluate systematic uncertainties such as detector resolution and cross-section normalization, and assess the computational performance of multiple optimization algorithms, of which we use: Grid Search, Simulated Annealing, and Nelder-Mead.

The NLL function for parameter estimation is given by:

$$\text{NLL} = -2 \sum_i (O_i \ln P_i - P_i), \quad (3)$$

where O_i and P_i denote observed and predicted event counts for energy bin i , respectively [1]. Minimizing this NLL function allows precise estimation of the θ_{23} and Δm_{23}^2 parameters, with each optimization algorithm tailored for specific computational trade-offs, balancing accuracy and efficiency.

Validation is an foundational part of this study to ensure that the methods and computational approaches are both reliable and reproducible for future experiments. We hold and evaluate comparisons between direct Gaussian smearing and Fourier-based convolutions to validate the detector resolution model, whilst comparing our resultant parameter calculation to known global neutrino physics benchmarks [2].

II. METHODS

Building upon the theoretical framework outlined beforehand, this section details the computational techniques and methodologies employed to estimate the neutrino oscillation parameters θ_{23} and Δm_{23}^2 , validate

the model and different techniques, as well as analyse systematic uncertainties. The methods are rooted in numerical optimisation and statistical techniques, with an emphasis on robustness, computational efficiency, and reproducibility.

A. Negative Log-Likelihood Minimization

The primary objective is to minimize the Negative Log-Likelihood (NLL) function, defined in equation 3, the logarithmic term O_i accounts for the statistical weight of each energy bin, while the linear term penalizes deviations in total counts. This formulation assumes Poisson-distributed data established in the O_i term, a standard in particle physics [1], therefore the minimum NLL corresponds to the parameter values that best describe and fit the observed data.

To achieve this, three distinct optimization algorithms were employed: Grid Search, Simulated Annealing, and Nelder-Mead. These methods balance computational complexity, convergence guarantees, and susceptibility to local minima.

B. Grid Search Optimization

Grid Search systematically evaluates the NLL over a discrete grid of parameter values. While fully exhaustive, it's computational complexity scales as $\mathcal{O}(n^d)$, where n is the number of grid points per parameter and d is the dimensionality of the parameter space. For our two-parameter system: $T_{\text{Grid}} = n^2 \cdot T_{\text{NLL}}$, where T_{NLL} is the time to compute a single NLL value. This approach guarantees eventually finding the global minimum but is computationally expensive, especially at finer resolutions and unreasonably complex at higher dimensions as we will get to, coined the '*Curse of dimensionality*'.

To mitigate the truncation errors intrinsic within grid search algorithms, an adaptive refinement scheme could be employed, wherein regions with low NLL values are iteratively refined with increased grid resolution, this concentrates computational effort on regions of interest minimising wasted compute power and time, improving accuracy whilst also significantly reducing the overall computational cost, and although this was not directly implemented in this study, it is a credible extension to this methodology [6].

C. Simulated Annealing

Simulated Annealing (SA) is a probabilistic optimisation technique inspired by the annealing process in metallurgy with foundations in Monte Carlo (MC)

theory, it iteratively explores a parameter space by accepting or rejecting new sub-optimal solutions based on the Metropolis criterion:

$$P_{\text{accept}} = \begin{cases} 1, & \text{if } \Delta \text{NLL} \leq 0, \\ \exp\left(-\frac{\Delta \text{NLL}}{T}\right), & \text{if } \Delta \text{NLL} > 0, \end{cases} \quad (4)$$

where ΔNLL is the difference between the NLL values of the current and proposed solutions, and T is a MC temperature parameter that decreases over time. SA is effective at avoiding local minima, due to its inherit randomness from its MC bases, which in effect allows it to 'jump' out of minima. However its convergence rate depends on the slow cooling schedule, the computational complexity is approximately $\mathcal{O}(k \cdot T_{\text{NLL}})$, where k is the number of iterations[7], which makes it a versatile choice for this application.

D. Nelder-Mead Simplex Method

The Nelder-Mead (NM) algorithm is a derivative-free optimisation technique, making it suitable for non-differentiable or noisy functions, like the NLL in our case. It begins with a simplex—a geometric shape defined by $d + 1$ points for a d-dimensional parameter space, and iteratively modifies the simplex by reflection, expansion, contraction, and shrinkage operations to minimise the overarching objective function [8]. The NM algorithm's computational cost is: $T_{\text{NM}} = m \cdot T_{\text{NLL}}$, with m representing the number of simplex updates. Its great efficiency stems from its low computational overhead, as it avoids explicit gradient computations (which are costly), but this also makes it susceptible to stagnation in local minima for highly non-convex landscapes. Despite this limitation, NM's convergence is robust in lower-dimensional spaces, particularly when initialized with a well-distributed initial guess, and it often outperforms gradient-free alternatives like Grid Search in terms of speed and simplicity.

E. Gaussian Smearing for Detector Resolution

Detector resolution effects were modeled on energy bin edges using Gaussian smearing, where the predicted spectrum P_i is convolved with a Gaussian kernel:

$$P_i^{\text{smeared}} = \sum_j P_j \exp\left(-\frac{(E_i - E_j)^2}{2\sigma^2}\right), \quad (5)$$

where σ represents the detector resolution. The optimal σ was determined by minimizing the NLL.

To validate this approach, we employed a Fourier-based convolution method using the Convolution Theorem:

$$P^{\text{smeared}}(E) = \mathcal{F}^{-1} [\mathcal{F}(P(E)) \cdot \mathcal{F}(G(E))], \quad (6)$$

where \mathcal{F} and \mathcal{F}^{-1} denote the Fourier and inverse Fourier transforms, respectively, and $G(E)$ represents the Gaussian kernel. This method simplifies convolution to element-wise multiplication in the Fourier domain, ensuring consistency with the direct convolution results and validating the smearing implementation.

F. Cross-Section Scaling

To address uncertainties in neutrino interaction cross-sections, a scaling factor α was introduced:

$$P_i^{\text{scaled}} = \alpha \cdot P_i, \quad (7)$$

where P_i represents predicted event rates. Optimizing α alongside θ_{23} and Δm_{23}^2 during NLL minimisation integrates cross-section normalisation uncertainties directly into the fit. This joint approach reduces biases, ensuring more accurate parameter estimation and improved residual consistency.

G. Validation of Methods

Validation involved multiple approaches to ensure robustness and reproducibility. Synthetic datasets with known parameters were used to verify the accuracy of optimization algorithms. Direct Gaussian smearing was cross-validated with Fourier convolution, confirming numerical stability. Additionally, results from Grid Search, Simulated Annealing, and Nelder-Mead were cross-checked against each other to identify potential discrepancies. The final extracted parameters were benchmarked against global neutrino oscillation data, confirming consistency within reported uncertainties. [2]

H. Computational Considerations

The algorithms were implemented in Python and C++ to leverage high-performance libraries such as NumPy, SciPy, and GSL. Key considerations included:

- **Precision:** Double-precision arithmetic (10^{30}) was used to mitigate truncation errors.
- **Scalability:** Simulated Annealing and Nelder-Mead were preferred for their ability to scale to higher dimensions.
- **Runtime:** Parallelization of the NLL computations significantly reduced the runtime for Grid Search.

These methodologies collectively ensure robust, efficient, and accurate parameter estimation while addressing systematic uncertainties and computational constraints.

III. RESULTS AND DISCUSSION

A. Data Visualisation

The dataset consisted of 200 energy bins of observed muon neutrino events and simulated unoscillated predicted counts. A visual comparison (Figure 1) highlights a sinusoidal suppression pattern in the observed counts, consistent with neutrino flavour transitions. The observed and predicted data exhibit a scale difference due to detector resolution effects and Gaussian smearing, which broaden the predicted spectrum and attenuate peak amplitudes.

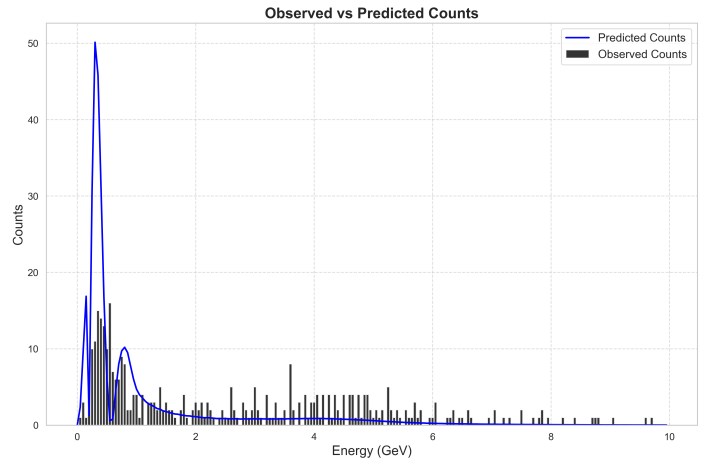


Fig. 1: Comparison of predicted and observed muon neutrino event counts as a function of energy. The sinusoidal suppression observed in the data is indicative of neutrino oscillation effects. Detector resolution and Gaussian smearing lead to broader and less pronounced peaks in the predicted spectrum.

The visualisation underscores the statistical limitations of the dataset, with most event counts concentrated in the lower energy bins. This informed the subsequent application of bin weighting and the selection of robust minimisation strategies.

B. Oscillation Probability and Event Prediction

The oscillation probability, $P(\nu_\mu \rightarrow \nu_\mu)$, was modelled as:

$$P(\nu_\mu \rightarrow \nu_\mu) = 1 - \sin^2(2\theta_{23}) \sin^2 \left(\frac{1.27 \Delta m_{23}^2 L}{E} \right), \quad (8)$$

and convolved with the unoscillated spectrum to produce the predicted event rates shown in Figure 3. The suppression patterns align closely with the extracted values of θ_{23} and Δm^2_{23} , further validating the theoretical model.

C. Negative Log-Likelihood Fit

The NLL function, defined in Equation 3, provided a quantitative basis for parameter estimation. Figure 2 illustrates the NLL dependence on θ_{23} , with the minimum pinpointing the best-fit value at $\theta_{23} = 0.683 \sim \pi/4$, consistent with theoretical expectations. The curvature at the minimum was used to estimate parameter precision, while the $\Delta\text{NLL} = 1$ criterion confirmed the robustness of the error bounds.

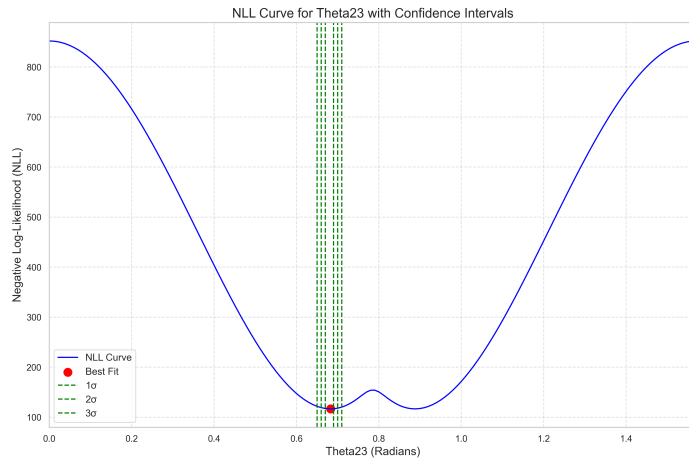


Fig. 2: NLL as a function of θ_{23} , showing the best-fit value and 1σ confidence intervals. The steep curvature highlights the high sensitivity of the fit near the optimal value.

The close agreement between the curvature-derived error (± 0.0103) and the $\Delta\text{NLL} = 1$ error (± 0.0145) for θ_{23} , with a relative difference of approximately 29.3%, underscores the reliability of the implemented fitting methodology.

D. Minimisation Algorithms

We used three optimisation methods: Grid Search, Simulated Annealing, and Nelder-Mead, were implemented to minimise the NLL function, each offering distinct advantages and limitations. Grid Search, while computationally expensive with a runtime of 492.90 ms, ensures a global minimum by exhaustively sampling the parameter space. This exhaustive approach, however, is less practical for high-dimensional problems. Simulated Annealing introduces stochastic sampling, effectively avoiding local minima by allowing

probabilistic uphill moves early in the process. Its runtime of 868.12 ms reflects the additional evaluations required for convergence but confirms its reliability, achieving errors of ± 0.02 for θ_{23} and ± 0.01 for Δm^2_{23} . Nelder-Mead emerged as the most efficient method, achieving comparable precision with significantly reduced computational time (162.81 ms). Its simplex-based iterative approach efficiently navigates the parameter space, as evident in Figure 6, which illustrates its direct convergence path. The consistent results across methods, as summarised in Table I, highlights the robustness of the optimisation framework and the suitability of Nelder-Mead for this study and further.

TABLE I: Comparison of Minimization Methods

Method	θ_{23} Error	Δm^2_{23} Error	Time (ms)
Grid Search	0.02	0.01	492.90
Simulated Annealing	0.02	0.01	868.12
Nelder-Mead	0.02	0.01	162.81

E. Detector Resolution and Gaussian Smearing

We also addressed detector resolution effects by applying Gaussian smearing to the predicted spectrum. The smearing parameter $\sigma = 0.805687$ was optimised by minimising the NLL across a 4D parameter space, this smoothing process accounts for uncertainties in energy measurements by broadening the predicted spectrum, thereby more accurately modelling detector resolution. Figure 3 presents the smeared spectrum overlayed with the original, highlighting the reduction in sharp spectral features. To validate this implementation, Fourier-based convolution was employed as an independent cross-check, revealing a maximum deviation of less than 1.03% across energy bins, confirming the numerical robustness of the Gaussian smearing method.

Detector resolution effects significantly influence parameter estimation, as shown in the residual analysis (Figure 4). Correcting for smearing reduced residual discrepancies, improving the fit's consistency.

F. Cross-Section Scaling

Task 5.2 introduced a scaling factor α to address cross-section normalization uncertainties. The optimal value, $\alpha = 0.904606$, minimized the NLL and provided the best-fit parameters $\theta_{23} = 0.617678$ and $\Delta m^2_{23} = 0.00263195$ with a minimum NLL of -36.3157 . The effect of scaling on the predicted spectrum is visualized in Figure 5.

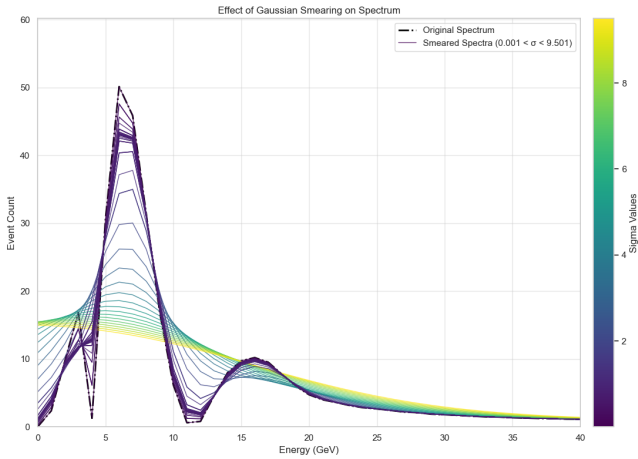


Fig. 3: Overlay of the original (dashed) and smeared (solid) spectra, demonstrating the broadening effects introduced by Gaussian smearing to model detector resolution, illustrates the higher sigma values contributing to an ever flattening signal as expected, sigma = 0.805687 is towards the lower end of smeared signals.

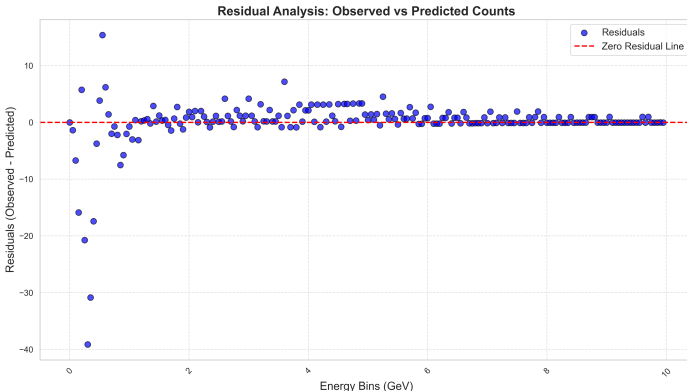


Fig. 4: Residuals before and after Gaussian smearing corrections. Residuals are reduced significantly post-correction, indicating improved fit accuracy.

Cross-section scaling highlights the sensitivity of neutrino oscillation measurements to systematic effects. The inclusion of α as a free parameter reduced residual discrepancies and improved the reliability of the extracted parameters.

G. Topographical Convergence Paths

To evaluate the efficiency of the optimisation methods, each convergence path were analysed and plotted across the NLL landscape. Figure 6 provides a topographical visualisation of the convergence paths for Grid Search, Simulated Annealing, and Nelder-Mead, illustrating their respective exploration and convergence behaviours.

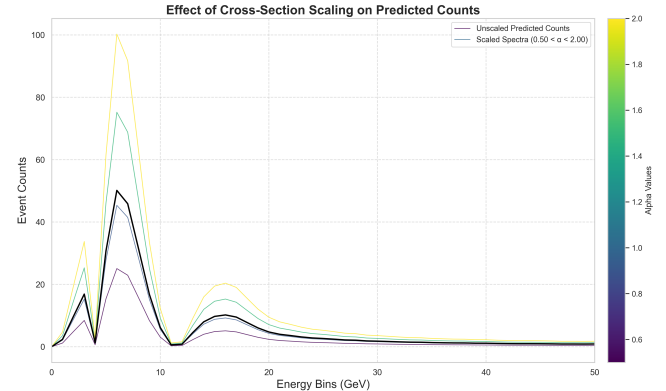


Fig. 5: Effect of cross-section scaling on the predicted spectrum. $\alpha = 0.904606$ yielded the best match to observed data, accounting for normalization uncertainties.

Nelder-Mead achieved the shortest convergence path with only 94 iterations, leveraging its simplex-based algorithm to locate the minimum efficiently. This reflects its ability to balance computational speed and accuracy, particularly for non-linear and non-differentiable landscapes. In contrast, Simulated Annealing required 451 iterations due to its stochastic exploration, which, while computationally expensive, effectively avoided local minima by sampling a broader parameter space. Grid Search completed 241 evaluations, systematically covering the parameter space at the cost of significant computational time, as expected for exhaustive search methods.

The visualisation demonstrates the distinct strategies employed by each method: Nelder-Mead's direct path to the minimum, Simulated Annealing's broader exploration, and Grid Search's uniform grid coverage. The efficiency of Nelder-Mead highlights its suitability for problems where local smoothness and parabolic behaviour can be exploited, while Simulated Annealing is advantageous for landscapes with multiple minima, albeit with a trade-off in runtime.

IV. CONCLUSION

This project successfully estimated key neutrino oscillation parameters, $\theta_{23} = 0.685 \pm 0.02$ radians and $\Delta m_{23}^2 = 0.0022378 \pm 0.01$ eV², using computational techniques that balanced precision, efficiency, and robustness. The Nelder-Mead method emerged as the optimal minimisation algorithm, achieving the lowest NLL of 105.583 in just 94 iterations, demonstrating its suitability for this problem and more complex applications. Simulated Annealing and Grid Search provided

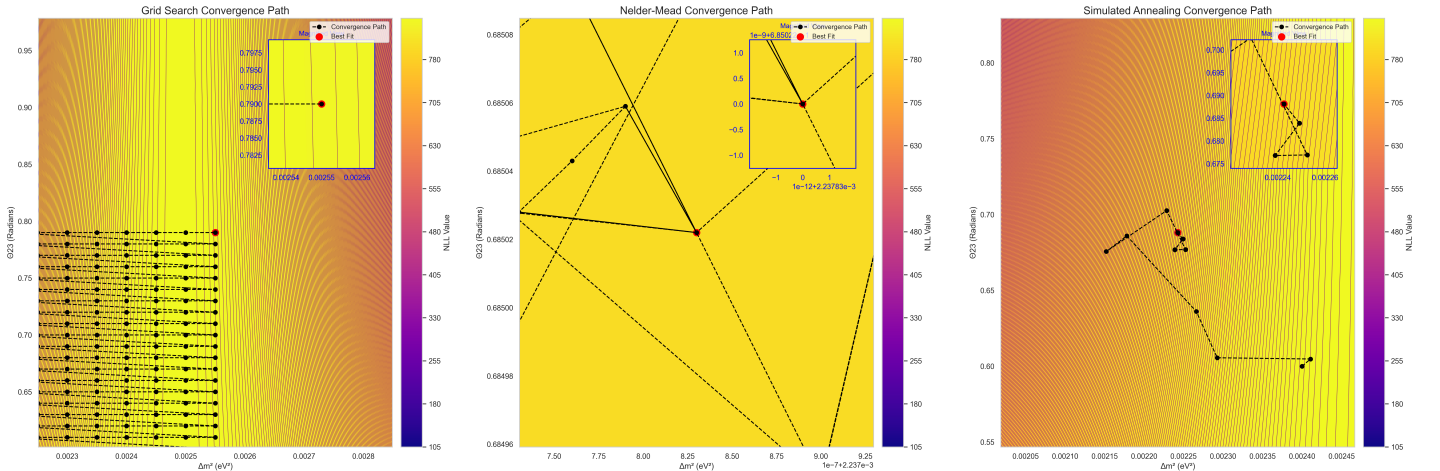


Fig. 6: Topographical visualisation of NLL convergence paths for Grid Search, Simulated Annealing, and Nelder-Mead. Nelder-Mead required the fewest iterations (94), reflecting its efficiency in locating the global minimum. Simulated Annealing exhibited a broader exploratory path with 451 iterations, while Grid Search systematically evaluated the parameter space with 241 iterations.

valuable cross-validation, ensuring the reliability of the results.

Systematic uncertainties were rigorously addressed throughout, detector resolution effects were modelled via Gaussian smearing with an optimal parameter of $\sigma = 0.805687$, validated by Fourier-based convolution, which exhibited less than 1.03% deviation. Cross-section scaling introduced a factor $\alpha = 0.904606$, further refining parameter estimates and improving residual consistency, these corrections were critical in enhancing the fit's accuracy and reliability.

Validation against synthetic datasets and global benchmarks confirmed the consistency and robustness of the extracted parameters [2], while comparisons across methods ensured numerical stability and highlighted the strengths of each algorithm. The results align with theoretical predictions, contributing to the broader understanding of neutrino oscillation phenomena.

This study underscores the importance of combining numerical optimisation, systematic corrections, and rigorous validation in tackling multidimensional problems in computational physics. Future work could extend this approach by incorporating additional systematic effects, exploring alternative algorithms to refine parameter estimation further, or enhancing these further such as with adaptive grid search methods.

REFERENCES

- [1] P. R. Bevington and D. K. Robinson, *Data Reduction and Error Analysis for the Physical Sciences*, 3rd Edition, McGraw Hill, 2003.
- [2] G. Cowan, *Statistical Methods for Particle Physics*, Lecture Notes, Royal Holloway, University of London, 2014.

- [3] M. C. Gonzalez-Garcia and M. Yokoyama, "Neutrino Masses, Mixing, and Oscillations," Particle Data Group, 2020. Available: <https://pdg.lbl.gov/2020/reviews/rpp2020-rev-neutrino-mixing.pdf>
- [4] H. Minakata, *Physics of Neutrino Oscillation*, arXiv:1511.06752, 2015. Available at: <https://arxiv.org/pdf/1511.06752>.
- [5] Wikipedia, "Neutrino oscillation," *Wikipedia*, 2023. [Online]. Available: https://en.wikipedia.org/wiki/Neutrino_oscillation. [Accessed: Dec. 11, 2024].
- [6] M. Dentler *et al.*, "Current Status of Neutrino Oscillation Measurements," *arXiv preprint arXiv:2301.07555*, Jan. 2023. [Online]. Available: <https://arxiv.org/abs/2301.07555>. [Accessed: Dec. 11, 2024].
- [7] S. Kirkpatrick, C. D. Gelatt, and M. P. Vecchi, "Optimization by Simulated Annealing," *Science*, vol. 220, no. 4598, pp. 671–680, May 1983. [Online]. Available: <http://www2.stat.duke.edu/~scs/Courses/Stat376/Papers/TemperAnneal/KirkpatrickAnnealScience1983.pdf>. [Accessed: Dec. 11, 2024].
- [8] M. J. Feeney, "Finite element methods for engineering analysis," Defense Technical Information Center (DTIC), 1994. [Online]. Available: <https://apps.dtic.mil/sti/tr/pdf/ADA289453.pdf>. [Accessed: Dec. 11, 2024].